

Electronic Structure Calculations of Organic-Metal Interfaces: A First-Principles Study

Rachid Belkada^{1,2}, Yoshiyuki Shirakawa², Masanori Kohyama³,
Jusuke Hidaka² and Shingo Tanaka³

¹Kyoto Prefecture Collaboration of Regional Entities for the advancement of Technological Excellence,
Japan Science and Technology Agency, 1-7 Hikaridai, Kyoto 619-0237, Japan,

Fax: 81-774-98-2214, e-mail: rbelkada@kcoe.jp

²Department of Chemical Engineering and Materials Science, Doshisha University,
1-3 Kyotanabe, Kyoto, 610-0321, Japan,

³Material Science Research Group, Research Institute for Ubiquitous Energy Devices,
National Institute of Advanced Industrial Science and Technology,
1-8-31, Midorigaoka, Ikeda, Osaka 563-8577, Japan

This article presents a first-principles study on sub-microscopic interaction between small organic molecules with the metal surface. We investigate the ground state electronic properties of a short alkane; (pentane-C₅H₁₂)-Al interface and that of a short Poly-Tetra-Fluoro-Ethylene (PTFE)-Al interface, using a recently developed RMM-DIIS scheme parallelized with respect to each band. The present results indicated that, the on-top crystallographic site “the carbon atom of the molecule located on top of the Al atom” is energetically more stable than other sites for both C₅H₁₂/Al and C₅F₁₂/Al systems at different interface distances.

Key words: density functional method, organic-metal interface, parallel computing, energy minimization techniques, organic molecules.

1. INTRODUCTION

In spite to the rapid development of organic electronic devices, the detail fundamental study of organic/metal interfaces become recently very important and an attractive one. The objective of the current work is to use efficient simulation techniques based on the density functional method (DFT) [1] to study the electronic structure properties of two interfaces formed between a metal and a short alkane;(C_nH_{2n+2}) or a short poly-tetra-fluoro-ethylene;(C_nF_{2n+2}) considering several geometrical orientations of the organic molecules on metal surface.

It is well known that performance of devices containing organic/metal interfaces is governed by their electronic and structural properties. Thus, the knowledge of sub-microscopic interaction at the interface between an organic material and a metal is enormously important for both understanding the mechanism of interface phenomenon and for applications. The C_nH_{2n+2} and its analogous material C_nF_{2n+2} obtained from substituting F by H atoms are basic materials in organic chemistry. The C_nH_{2n+2} is a widely studied polymer having a planar atomic configuration between C and two H atoms. Due to the steric hindrance among F atoms, the C_nF_{2n+2} chain adopt a helical structure with 3 helix in normal condition [2]. The study of these 2 fundamental prototype systems offer a chance to understand the mechanisms of dipole formation at

the organic insulator-metal interfaces which is very important to consider how to treat band alignments at other typical organic-metal systems.

The preliminary results for C_nH_{2n+2}/Al interface indicated that, the CH₂ group near to the interface is physisorbed without strong interaction. However, even for the typical organic insulator C_nF_{2n+2}/Al system an interface dipole layer can be formed not due to image effect but possibly resulted from a small chemical interaction. In connection to the present study, a recent experimental investigation by NEXAFS technique on C₄₄H₉₀/metal system indicated a formation of metal induced gap states [3] for such interface. There exist several possible reasons behind the origin of dipole formation between an organic molecule and a metal surface. Ignoring the mechanism of dipole formation will lead to a lack in controlling device performance and affect the design of novel devices.

2. CALCULATION METHOD

Interface phenomena occurring between an organic molecule and a metal surface are often complex and they require a robust simulation methodology. In the present work we use a recently developed parallelization scheme for plane-wave pseudopotential method based on the DFT within the local density approximation [1] to calculate the electronic ground state of large systems efficiently [4,5].

The total energy is calculated using the well known Kohn-Sham (KS) functional [1], which depends on the positions of the ions and the electronic wave functions. Under the constraints of orthogonalization, variation with respect to the wave functions leads to KS eigenvalue problem [1] given as follow:

$$H|\psi_i\rangle = \varepsilon_i|\psi_i\rangle \quad (1)$$

In plane-wave pseudopotential method [6] obtaining efficiently the electronic ground state requires solving iteratively equation (1) in a self-consistent manner. In usual iterative scheme such as conjugate gradient (CG) algorithm, the self-consistent calculation is performed for several CG steps and starts from an arbitrary given wave function ψ_i^m at state i . In the next CG iteration the new trial wave function ψ_i^{m+1} is constructed by considering only the previous ψ_i^m vector and its conjugate. The electronic ground state is obtained through iterative update of the wave functions so as to lower the expectation eigenvalue (ε_i) of the Hamiltonian (H) in equation (1) for each CG step.

In the former scheme, parallelization with respect to each k point is efficient and rather easy to implement as discussed in BKL-CG [7] method. However, when dealing with large system the CG scheme is not convenient due to frequent orthogonalization operations among wave functions resulting in a large data transfer between processors. An alternative approach proposed by Pulay [8] for electronic optimization is the Residual Minimization Method-Direct Inversion in the Iterative Subspace (RMM-DIIS) scheme, which is more suited for parallelization with respect to each band than the other minimization schemes [5].

Iterative matrix diagonalization in RMM-DIIS scheme involve update of a given trial vector ψ_i^m and a determination of a residual (R) associated with the vector as defined in (2). At each iterative step, the DIIS minimization scheme works with a limited set of $\{\psi_i\}$ vectors.

$$|R_i\rangle = (H - \varepsilon_i)|\psi_i\rangle \quad (2)$$

$$|\overline{\psi}^M\rangle = \sum_{i=0}^M \alpha_i |\psi_i^m\rangle \quad \text{with } M=1 \quad (3)$$

In going from one step to the next one, a new vector; ψ_i^{m+1} is generated from both the residual (R) and the previous vector as to lower the energy expectation value. Next, as given in equation (3) a linear combination of the initial vector ψ_i^m and the new trial wave function ψ_i^{m+1} is determined as to minimize the norm of the residual vector. In this scheme each wave function is updated so as to minimize its residual vector, and each wave function converges to the wave function of the no residual nearby, namely the eigenstate nearby, without explicit orthogonalization. After a run through all the bands for each k points, the total energy and the Hellmann-Feynman [9] atomic forces are calculated for each step of atomic

motion through the calculation of the electronic ground state. In the present paper rather underlying ideas of the methodology are presented. A more rigorous description can be found in the original paper [4-10].

To reduce the computation cost by decreasing the number of plane-wave, a soft-type norm-conserved pseudopotential developed by Troullier-Martins [11] is used, for C, F, and Al elements. For the case of H element we use the norm-conserved Hamann type pseudopotential [12]. The pseudopotentials for C_5H_{12} molecule are constructed from $2s^22p^2$ and $1s^12p^0$ electronic configurations respectively for C and H elements with the p and s potentials as local components for C and H, respectively. For s and p orbital of C element we adopt cutoff radii of 1.44 (a.u), and for H element we use a value of 0.42 (a.u) for s orbital. In the case of C_5F_{12} molecule we use the recently optimized pseudopotential for F examined in the study of structural optimization of $\alpha-AlF_3$ [13]. This pseudopotential are generated from $2s^22p^5$ configuration with cutoff radius of 1.3 (a.u) for both s and p orbital selecting s orbital as a local component. The properties of these pseudopotentials are well examined to reproduce accurately the C-H and C-F bond distances in C_5H_{12} and in C_5F_8 molecules, respectively. The pseudopotential of Al element is generated from $3s^13p^{0.5}3d^{0.5}$ electronic configuration with the cutoff radii of 1.8 (a.u) for s and 2.0 (a.u) for both p and d orbital and selecting p orbital as a local potential. The present pseudopotential has been used to well reproduce the bulk and interface properties in SiC-Al interface [14].

In this work, for each supercell of Al(110)/ C_5H_{12} and Al(110)/ C_5F_{12} system, the slab contains five Al-layers and connect vertically to either C_5H_{10} or C_5F_{10} molecules. These two molecules are capped at their two extremities by either F or H termination atoms. The unit cell include in total 37 atoms for each system and the size of the cell is of 16 X 11 X 50 (a.u) which include enough vacuum region along z axis to avoid artifacts in the calculation. For the update of the charge density in the iterations step we adopt the Pulay mixing scheme [8]. A plane-wave cutoff energy of 30 (Ry) was used, requiring 22421 plane waves. 4 k points per half of the Brillouine zone are used with 0.2 (eV) for Gaussian broadening scheme. The electronic structure is studied using respectively 58 and 100 bands for Al/ C_5H_{12} and Al/ C_5F_{12} systems. Update of a wave function by RMM-DIIS method is stopped if the change in total eigenvalue becomes smaller than 30% of its initial value, or if the change in total eigenvalue becomes smaller than 10^{-7} (Ry).

3. RESULTS AND DISCUSSION

At first it is necessary to check the reliability of the present pseudopotentials for Al, C, F, and H elements to correctly reproduce the structural and electronic properties of C_5H_{12} , C_5F_{12} molecules and Al(110) surface. For this purpose we perform structural optimization by atomic relaxation of the

molecules and Al slab surface in the supercell as defined previously. Due to large computational effort, the pseudopotential for F element is tested using a small molecule; C_3F_8 in order to reduce the computational effort.

The initial atomic position for C, H and F are obtained from experimentally observed bond distance and bond angles cited in [2,15], which are indicated in Table I. In the calculation all the atoms in C_5H_{12} and C_3F_8 molecules are fully relaxed by the exact Hellmann-Feynman forces till their maximum values in x, y, and z are less than 0.1 eV/Å. Table I shows the obtained results using RMM-DIIS scheme after free atomic relaxation, which indicate a good agreement with other experimental results and reproduce well the local atomic configuration of both molecules.

Table I. Optimized bond distances and bond angles for C_5H_{12} and C_3F_8 molecules.

Molecules	Experimental*	Relaxed**	
C_5H_{12}	C-H (Å)	1.05	1.124
	C-C(Å)	1.53	1.511
	C-C-C	112°	113.7°
	H-C-H	107°	106.7°
C_3F_8	C-F(Å)	1.34	1.35
	C-C(Å)	1.54	1.52
	C-C-C	115°	112.5°
	F-C-F	104°	107.1°

*) listed in [2] for C_nH_{2n+2} and in [15] for C_nF_{2n+2} .
**) present method.

Before performing relaxation of Al(110) surface, we have optimized the lattice constant of Al bulk starting from the experimental value. The obtained equilibrium lattice constant is determined to be 0.395 nm, which is consistent with the results from the recent LDA prediction [16] and experimentally observed value of 0.402 nm at 0 K [17]. Next we prepare a slab model for Al(110) surface calculation. The supercell of the slab contains nine Al(110) layers, all atoms in the slab are fully relaxed till the maximum values of the atomic forces in x, y, and z are less than 0.2 eV/Å.

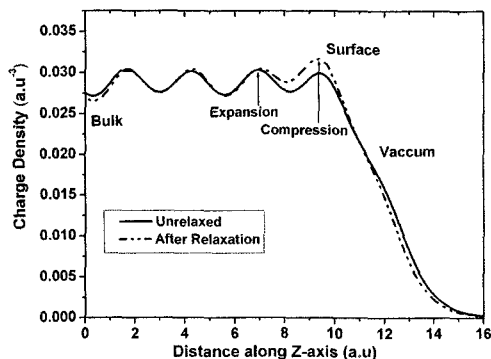


Fig.1. Multilayer relaxations of clean Al(110) surface. The charge density in the slab is plotted from the bulk to the vacuum region for nine Al-layers.

Figure 1, shows the result obtained from surface multilayer relaxations for Al(110) surface. Our calculation predict well the inward relaxation feature of Al(110) surface, which is consistent with other DFT calculations [16,18] and experimental study by low energy electron diffraction (LEED) method [19]. The inward relaxation of the top atom layer induces a compression of the interlayer distance between first and the second atomic layer resulting in the charge density increases between these two layers as shown in Fig. 1. A possible explanation of inward relaxation mechanism of Al(110) surface is a consequence of bond order bond length correlation. The surface atoms lose several neighbors due to the surface formation, which cause electronic redistribution at the surface and strengthen bonding between the first and second atomic layers, thus leading to an inward relaxation.

Table II compares the results from the present multilayer relaxation with other LDA calculations performed using different slab size and results from experimental observation. The interlayer spacing is indicated by Δ_{ij} , which is calculated by the percentage change in the interlayer distance between layer i and layer j as compared to initial bulk interlayer distances.

Table II. Interlayer distances after relaxation of clean Al(110) surface using the present Al pseudopotential.

	Relaxation (%)			
	Δ_{12}	Δ_{23}	Δ_{34}	Δ_{45}
Present method	-9.43	1.62	-1.53	1.60
LDA ^a	-6.10	5.50	-2.2	1.70
LDA ^b	-7.68	5.15	-0.85	3.21
Experiment ^c	-8.5	5.5	-1.6	1.0

^a) Slab model with 8 Al-layers [16], ^b) Calculation using 11 Al-layers slab model [18] and ^c) From LEED [19].

Using the presently tested pseudopotentials we have performed a search for lowest energy configuration of C_5H_{12}/Al and C_5F_{12}/Al interfaces. The initial configurations of the molecules over the Al(110) surfaces were set by translating the molecule rigidly along the (001) plane of the metal surface. For the Al(110) surface there exist four special positions that the molecules C_5H_{12} or C_5F_{12} can occupy, corresponding to extrema on the energy surface. These are the on-top site over the surface atom, on-top site over the first atom below the surface, the short bridging site, the long bridging site. Each of these sites was tested to determine the lowest energy position of adsorbed molecules. For each system, calculations are performed at different interface distances.

Figure 2 and 3 shows respectively the averaged potential curves of C_5H_{12}/Al and C_5F_{12}/Al systems obtained along the direction normal to the interfaces, which are plotted starting from the center of Al slab. The averaged potential is calculated from the summation of the local component of pseudopotential, the Hartree

potential, and the exchange-correlation potential averaged on each plan parallel to the surface. The non-local part of the pseudopotential existing only near atoms is neglected because of no long-range effects. In Fig.2 and 3 the energy levels for the highest occupied molecular orbital (HOMO) and the lowest unoccupied molecular orbital (LUMO) are also included, which are calculated from the individual isolated C_5H_{12} and C_5F_{12} molecules.

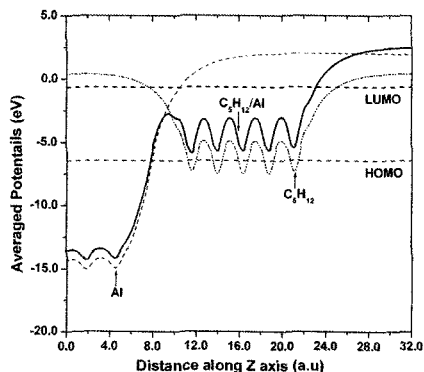


Fig.2. Averaged potential profiles, in dashed line for clean Al(110) slab surface and isolated C_5H_{12} molecule, for C_5H_{12}/Al interface (solid line).

For the C_5H_{12}/Al system the on-top site at the interface distance of 0.3 nm correspond to the lowest-energy position. At this interface distance we obtained the averaged potential profile as shown in Fig.2. In this figure the position of the interface is obtained from the intersection of clean Al surface potential with that of isolated C_5H_{12} molecule and we set the potential at this point to be as a reference before contact. After the interface is formed the C_5H_{12} potential raise without large change in the interface potential as compared to the

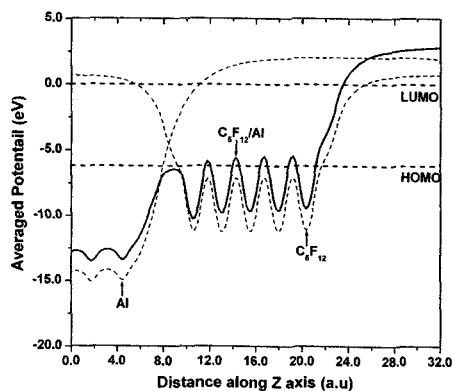


Fig.3. Averaged potential profiles in dashed line for clean Al(110) surface and isolated C_5F_{12} molecule. The potential of C_5F_{12}/Al interface is in solid line.

situation before contact and the electronic structure of the organic layer is preserved, which can be explained by the physisorption character of this type of inert interface. On the other hand the large gradient in molecule side and in the vacuum

indicates the existence of large interface dipole layer beside the surface dipole layer. For the C_5F_{12}/Al system the minimum energy configuration at the interface distance of 0.25 nm also obtained when the C atoms is located on-top of Al atom. In this case the shift of the interface potential is more pronounced as indicated in Fig.3. Thus we can expect a small chemical interaction or charge transfer for this type of interface. A detailed electronic structure calculation are undergoing to resolve fundamental aspect of such wide HOMO-LUMO gap systems for understanding the mechanism responsible for the interface dipole layer formation.

ACKNOWLEDGEMENTS

The present work is supported by Kyoto Prefecture Collaboration of Regional Entities for the Avengement of Technological Excellence, JST. Calculations were performed using Super-Nova PC-cluster at Doshisha University and the IBM-JS20 e-server PC-cluster at Keihanna, Inc.

REFERENCES

- [1] P. Hohenberg and W. Kohn, *Phys. Rev.*, **36**, B871 (1964); W. Kohn and L. J. Sham, *Phys. Rev.*, **140**, A1138, (1965).
- [2] M. Springborg and M. Lev, *Phys.Rev.*, B **40**, 3333 (1989).
- [3] Y. Morikawa, H. Ishii, and K. Seki, *Phys. Rev.*, B **69**, 041403, (2004).
- [4] M. Kohyama, *Modeling Simulation Mater. Sci. Eng.*, 4397 (1996).
- [5] T. Tamura, G. Lu, R. Yamamoto, M. Kohyama, S.Tanaka and Y. Tateizumi, *Model. Simu. Mater. Sci. Eng.*, **12** 945 (2004).
- [6] M. C. Payne, M. P. Teter, D. C. Allan, T.A. Arias, and J. D. Joannopoulos, *Rev Mod. Phys.*, **64**, 1097 (1992).
- [7] D. M. Bylander, L. Kleinman, and S. Lee, *Phys. Rev. Lett.*, **48**, 1425 (1990).
- [8] P. Pulay, *J.Comp.Chem.*, **73**, 393 (1980).
- [9] R. P. Feynman, *Phys. Rev.*, **56**, 340 (1939).
- [10] G. Kresse and J. Furthmuller, *Phys. Rev.*, B **54**, 11168 (1996).
- [11] N. Troullier and J. L. Martins, *Phys. Rev.*, B **43**, 1993 (1991).
- [12] D. R. Hamann, M. Schluter and C. Chiang, *Phys. Rev. Lett.*, **43** 1494 (1979).
- [13] Y. R. Chen, V. P. and P. B. Allen, *Phys.Rev.*, B **69**, 054109 (2004).
- [14] M. Kohyama and J. Hokstra, *Phys. Rev.*, B **61**, 2672 (2000).
- [15] S. Kavesh and J. M. Schultz, *J. Polym. Sci.*, A2 **8**, 243 (1970).
- [16] N. Mazari, D. Vanderbilt, A. De Vita, M. C. Payne, *Phys. Rev. Lett.*, **82**, 3296 (1964).
- [17] G. N. Kamm, G. A. Albers, *J. Appl. Phys.*, **35**, 327 (1964).
- [18] J. C. Zheng H. Q. Wang, C.H. A. Huan, and A.T. S. Wee, *J. Electron. Spec. and Related Phenomena.*, **114** 501 (2001).
- [19] J. R. Noonan, H. L. Davis, *Phys.Rev.*, B **29**, 4349 (1984).